

Electron-hole conduction near the critical point of mercury

A. A. Likal'ter

Institute of High Temperatures, Russian Academy of Sciences, 127412 Moscow, Russia

(Submitted 6 July 1994)

Zh. Eksp. Teor. Fiz. **106**, 1663–1675 (December 1994)

Strongly collisional mercury vapor near the liquid-gas critical point is treated as a gaseous semiconductor with a weakly overlapping atomic structure. The permittivity is found to be anomalously large because in addition to the atomic polarization there is a contribution from interatomic bonds. The hole conductance involving superbarrier valence-electron transitions between ions and neighboring atoms, manifests itself in the positive sign of the thermoelectric power. The energy gap between the electron and hole bands is estimated using the dielectric screening model. According to the model there exists a connection between the dielectric anomaly, acting to reduce the gap, and the conductivity, which rises by a factor of 10^{10} compared to the ideal weakly ionized gas. © 1994 American Institute of Physics.

1. INTRODUCTION

Close to the critical point of the liquid-gas phase transition, metals also undergo a continuous metal-nonmetal transition involving the appearance of atomic structure. The interplay between these two types of transition has attracted attention for fifty years now.¹ Interest in this subject is being stimulated by the unusual electronic properties of the noble metals, not yet fully explained. Most of the information about these properties has been obtained for mercury, which enjoys a unique position among other metals. Among the metallic elements, mercury has the lowest critical temperature, $T_c=1751$ K, and the highest ionization potential, $I=10.44$ eV. The combination of these factors results in that the metal-nonmetal transition is accompanied by a relatively sharp conductivity drop.²

Since the conductivity remains finite, the metal-nonmetal transition point is located by the appearance (disappearance) of the activation energy. The linearly extrapolated activation energy vanishes at the density $\rho_{MN}=8.8$ g/cm³. Thus, the metal-nonmetal transition point in mercury is markedly above the critical density, $\rho_c=5.8$ g/cm³ (Ref. 3).

Assuming the existence of the atomic structure, the metal-nonmetal transition can be identified with the percolation threshold for the overlapping spheres in which the atomic wave functions are mainly concentrated.⁴ In the quasiclassical case, which is typical of metals, these are classically accessible spheres restricting the motion of valence electrons in atoms. Above the percolation threshold of the classically accessible spheres, the valence electrons can go from one atomic core to another above the potential barrier and so participate in conduction. Below the metal-nonmetal transition the conduction is by weakly excited electrons, for which the radius of the classically accessible sphere exceeds the percolation radius in the atomic gas. Such excitations occur due to the virtual screening of the atomic cores by the valence electrons of the neighboring atoms. When screening is included correctly, a simple quasiclassical percolation model of the metal-nonmetal transition is adequate to describe the electronic properties of extended metals.⁵ Note that microscopic percolation should be distinguished from

the macroscopic model of a heterogeneous continuous medium with metallic and nonmetallic regions as discussed in Ref. 6.

Experimentally (see the review article by Hensel *et al.*³ and references therein), even below the critical density (and down to 4 g/cm³) mercury displays typical semiconducting (rather than metallic) properties. The conductivity falls off with decreasing density, to well below its maximum metallic value, and at constant density grows exponentially with temperature. The dielectric permittivity is positive and has a value of from a few units to 10, typical of semiconductors. The thermoelectric power changes its sign to positive, indicative of hole conductance. All the signs are that in the density interval 4–6 g/cm³ at near-critical temperatures mercury vapor may be considered a gaseous semiconductor (in contrast, for example, to caesium vapor at the critical point, which is a gaseous metal). At still lower densities the dielectric permittivity drops to below 3 and the conduction mechanism changes again to become pure electronic, as usual in ionized gases.

For a thermally ionized gas of atoms with a high ionization potential, the conductivity of dense mercury vapor is anomalously high. In the case of a gaseous semiconductors, a possible explanation is the high permittivity, which reduces the ionization potential. The permittivity also behaves anomalously in departing strongly from the ordinary Clausius-Mosotti equation; close to the critical point it shows a strong temperature dependence.³ The permittivity anomaly is related to polarization of the bonds formed the overlapping atoms⁷ (an alternative suggestion is the increase in atomic polarizability due to excitation exchange⁸). The very sharp increase in permittivity with increasing pressure at constant temperature has prompted the phase transition idea. Most likely, however, the sharp permittivity and thermoelectric power changes result from their density dependence and from the divergence of the compressibility of the substance at the critical point.

In an intrinsic gaseous semiconductor the electrons excited into the conduction band move in the field of neutral atoms. Owing to the possibility of superbarrier transitions of the valence electrons from neighboring atoms to ions, mobile

holes appear at the ion positions. The occurrence of the superbarrier transitions and the presence of interatomic bonds responsible for the dielectric anomaly are a consequence of the metal-nonmetal transition (or, the other way around, presage a transition to the metallic state). Analysis of the various properties of a gaseous semiconductor clearly requires a general approach that includes the atomic structure in a fundamental way. Note that the vanishing of the thermoelectric power near the mercury critical point pointed to the electron-hole conductance idea even in the early work on the subject.⁹ However, the holes were assumed to be due to free-electron excitation across the Mott pseudogap (rather than atomic ionization). This hole concept neglects the strong electron-ion correlation and so has not received any further development.¹⁰

In the present paper a model is constructed of a gaseous semiconductor explaining (in principle) the change in the sign of thermoelectric power, and the conductivity of such a semiconductor is calculated. In parallel, a theory of anomalous dielectric permittivity is developed, with emphasis on a careful analysis of the number of interatomic bonds.

The plan of the paper is as follows. In Sec. 2, the conditions for the percolative hole mobility are discussed. In Sec. 3, a general discussion of electron-hole conduction in a gaseous semiconductor is contained. In Sec. 4, a dielectric model used to calculate the energy gap is formulated. In Sec. 5, a theory of anomalous permittivity is presented and used to estimate the conductivity. Finally, in Sec. 6 the thermoelectric power is discussed.

2. ELECTRON AND HOLE PERCOLATION

In mercury atoms the two valence electrons are in spherically symmetrical $6s$ states, whose radial wave functions have five nodes. The radial motion of the electrons is quasiclassical and is primarily restricted by the classically accessible sphere in the Coulomb potential of the singly charged atomic core. The radius of the sphere is e^2/I , where e is the electron charge and I the ionization potential of the atom. In an atomic gas each electron moves in the field of one atomic core, the remaining cores being screened by their own electrons. When the classically accessible spheres of neighboring atoms overlap, an electron may leave its atomic core to move to a virtually free atomic core (ion). Above the percolation threshold of the classically accessible spheres, the electron transitions between atomic cores cause diffusion. Moreover, the overlap of atoms leads to a virtual screening of the electron-ion interaction. Consequently, electron states in the overlapping atoms contain an admixture of free motion in a screened (atomic) potential.

Clearly, the admixture of free-electron states implies formation of an energy band in the spectrum of the overlapping atoms (quasiatoms). In particular, the minimum internal energy of a quasiatom, as measured from the energy of a singly charged ion, is defined by

$$E_p = -I + \varepsilon_p, \quad \varepsilon_p = p^2/2m, \quad (1)$$

where ε_p is the excitation energy, p the asymptotic free-motion momentum, and m the electronic mass. Taking ac-

count of excitation, the radius of the classically accessible sphere is $e^2/(-E_p)$, and the volume fraction of the spheres is

$$\zeta(E_p) = \frac{4\pi}{3} \left(\frac{e^2}{-E_p} \right)^3 n_a, \quad (2)$$

where n_a is the density of the atoms. The percolation threshold of weakly excited atoms is given by

$$\zeta(E_p) = \zeta_t, \quad (3)$$

where ζ_t is a parameter (for randomly arranged overlapping spheres, $\zeta_t \approx 1/3$). At the metal-nonmetal transition point the condition (3) holds for $\varepsilon_p = 0$:

$$\zeta_0 \equiv \zeta(-I) = \zeta_t. \quad (3')$$

The experimental value of the density, $\rho_{MN} = 8.8 \text{ g/cm}^3$, corresponds to $\zeta_t = 0.29$. Below the metal-nonmetal transition Eq. (3) determines the mobility gap

$$\Delta_t = I - e^2(4\pi n_a/3\zeta_t)^{1/3}. \quad (4)$$

Quasiclassical percolation of electrons is possible for excitation to above the mobility gap, i.e., for $\varepsilon_p > \Delta_t$. Furthermore, atoms may be treated as virtual ions only relatively close to the transition point, for example if

$$(\rho_{MN} - \rho)/\rho_{MN} < 1/3.$$

Thus, electronic percolation is practically possible only for mercury densities above the critical value.

The percolation threshold is lowered in the presence of bare ions. In fact, the unscreened potential of an ion, when added to the atomic core potential, reduces the potential barrier. Therefore the condition for an superbarrier transition of an electron from an atom to an ion is fulfilled at distances less than $4e^2/I$ (rather than $2e^2/I$ as in the two-atom case). Transitions of valence electrons to an ion are equivalent to the random walk (or diffusion) of a hole that occurs above the percolation threshold for spheres of radius $2e^2/I$. Thus, the hole diffusion threshold with respect to density is eight times lower than the metal-nonmetal transition point.

The extent to which the holes are free is characterized by the average number of bonds between an ion and the neighboring atoms in the absence of correlation:

$$B = \frac{4\pi}{3} \left(\frac{4e^2}{I} \right)^3 n_a. \quad (5)$$

The hole percolation threshold corresponds to the $B \approx 2.7$. At the critical mercury density this parameter reaches 12. In the limit of a large number of bonds the holes should be treated as free particles with the minimum mean free path possible.

In accord with the Ioffe-Regel criterion,¹¹ the minimum mean free path of the hole is limited by the quantum uncertainty in position,

$$l \geq \lambda_T, \quad \lambda_T = \sqrt{2\pi\hbar^2/mT}, \quad (6)$$

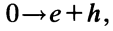
where l is the mean free path, λ_T is the average thermal wavelength, T is the temperature, and m is the hole effective mass. The same estimate follows from the energy-lifetime uncertainty relation for the hole,

$$\tau = l/v_T \geq \hbar/T, \quad (7)$$

where τ is the lifetime and $v_T = \sqrt{8T/\pi m}$ the average thermal velocity.

3. CONDUCTIVITY

In an intrinsic gaseous semiconductor holes result from the thermal excitation of the valence electrons into the conduction band. The excitation process can be represented as an electron-hole pair formation reaction,



the zero on the left corresponding to the ground state. The balance equation for this reaction is¹²

$$\mu_e + \mu_h = 0, \quad (8)$$

where μ_e and μ_h are the chemical potentials of the electrons and holes, respectively. The free-electron and free-hole densities are related to the chemical potentials by the expressions

$$n_e = \frac{2}{\lambda_T^3} \exp\left(\frac{\mu_e - \Delta}{T}\right) \quad (9)$$

and

$$n_h = \frac{2}{\lambda_T^3} \exp\left(\frac{\mu_h}{T}\right), \quad (10)$$

where Δ is the energy gap between the electron and hole bands. The electron and hole effective masses enter only the preexponential factors and may for simplicity be considered equal.

Multiplying Eq. (9) by Eq. (10) and using Eq. (8) we obtain

$$\sqrt{n_e n_h} = \frac{2}{\lambda_T^3} \exp\left(-\frac{\Delta}{2T}\right). \quad (11)$$

To find the free-carrier density one must consider the possibility of electrons and holes being trapped in fluctuation clusters (or bubbles). The electrical neutrality condition is then

$$n_e/a_e = n_h/a_h, \quad (12)$$

where a_e is the fraction of the free (untrapped) electrons, and a_h is that of the free holes. From Eqs. (11) and (12),

$$\frac{n_e}{a_e} = \frac{n_h}{a_h} = \frac{2}{\sqrt{a_e a_h} \lambda_T^3} \exp\left(-\frac{\Delta}{2T}\right). \quad (13)$$

Comparing Eq. (13) with expressions (9) and (10) we obtain the electron and hole chemical potentials:

$$\mu_e = -\mu_h = \frac{\Delta}{2} + \frac{T}{2} \ln \frac{a_e}{a_h}. \quad (14)$$

Finally, the total free-carrier density is

$$n = n_e + n_h = \frac{2}{\lambda_T^3} \left(\sqrt{\frac{a_e}{a_h}} + \sqrt{\frac{a_h}{a_e}} \right) \exp\left(-\frac{\Delta}{2T}\right). \quad (15)$$

Note that the asymmetric trapping of electrons and holes increases the total number of free carriers and that the minimum number of these corresponds to $a_e = a_h$:

$$n_m = \frac{4}{\lambda_T^3} \exp\left(-\frac{\Delta}{2T}\right). \quad (16)$$

The minimal conductivity is given by

$$\sigma_m = \frac{e^2 n_m \tau}{m} = \frac{e^2 n_m \lambda_T^2}{2\pi\hbar}, \quad (17)$$

where $\tau = \hbar/T$ is the minimum free lifetime. From Eq. (17), substituting the minimal free-carrier density (16), we have

$$\sigma_m = \frac{2e^2}{\pi\hbar\lambda_T} \exp\left(-\frac{\Delta}{2T}\right). \quad (18)$$

As usual, the conductivity depends exponentially on the width of the gap between the electron and hole bands. The preexponential factor in Eq. (18) at the critical temperature of mercury is of order $10^3 \Omega^{-1} \cdot \text{cm}^{-1}$. The actual conductivity is much lower, since the energy gap width is much larger than the temperature.

4. ENERGY GAP

The energy gap between the electron and hole bands is equal to the minimum electron-hole formation energy and depends on the free-atom ionization potential, the dielectric permittivity, and the structure of the atomic gas under study. A weakly excited valence electron moves in the Coulomb field of the atomic core

$$u = -e^2/r, \quad e^2/I < r < a, \quad (19)$$

where the radius a is on the order of the interatomic separation. For a strongly excited electron, the classically accessible sphere contains many atoms polarized by the core field. At distances larger than the interatomic separation, the potential has the form

$$u = -e^2/\epsilon_a r - (e^2/a)(1 - \epsilon_a^{-1}), \quad r > a, \quad (20)$$

where ϵ_a is the dielectric constant (Fig. 1). The additive constant in Eq. (20) [insuring a match with Eq. (19)] brings about a reduction in the atomic ionization energy. Thus the ionization energy is

$$\Delta = I - (e^2/a)(1 - \epsilon_a^{-1}).$$

Taking the limit $\epsilon_a \rightarrow \infty$ (corresponding to screening the potential completely for $r > a$) would formally extend this expression to the region near the metal-nonmetal transition point. Physically, in this limit the ionization energy must be just the mobility gap. But then comparison with Eq. (4) shows that the radius a must be equal to the percolation radius for overlapping atomic spheres. Neglecting long-range correlations between atoms and setting $\zeta_t \approx 1/3$, we have

$$a = (4\pi n_a)^{-1/3}.$$

Thus, the formula for the energy gap becomes

$$\Delta = I - e^2(4\pi n_a)^{1/3}(1 - \epsilon_a^{-1}). \quad (21)$$

In a gaseous semiconductor the magnitude of the gap depends on the density and temperature, including the implicit dependence via the permittivity.

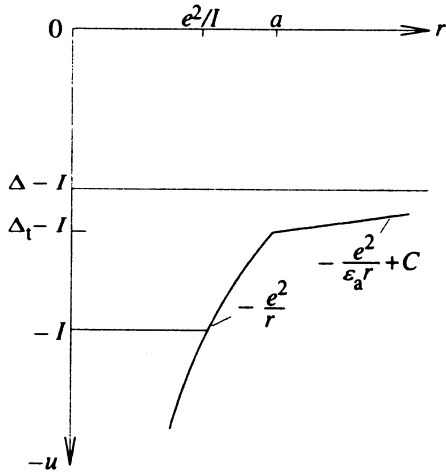


FIG. 1. Screened ion potential. Hatching indicates the conduction band bottom.

5. PERMITTIVITY

Close to its critical point mercury exhibits a large increase in permittivity, this property departing from the ordinary atomic-polarization formula of Clausius and Mosotti.³ This dielectric anomaly is due to the additional polarization of the interatomic bonds.⁵ In the quasiclassical case, atomic polarization reduces to a shift of classically accessible *s*-electron spheres. The polarization of interatomic bonds implies a partial transition of electrons between overlapping classically accessible spheres. The total polarizability per atom, including the interatomic bond polarizability, is

$$\alpha = \left(z + \frac{4}{3} C \right) \left(\frac{e^2}{I} \right)^3, \quad (22)$$

where *z* is the number of valence *s*-electrons in the atom and *C* is the number of bonds per atom.⁷

Twice the number of bonds per atom is given by the integral

$$2C = 4\pi n_a \int g(R) R^2 dR, \quad (23)$$

where *g*(*R*) is the radial distribution function and the region of integration is limited by a sphere of radius $2e^2/I$ (including tunneling increases the radius by $\sim (\hbar^2/2mI)^{1/2}$). This region encloses the first coordination sphere of the liquid, the average radius of which is about $3 \cdot 10^{-8}$ cm. Thus, the number of bonds per atom multiplied by two should be identified with the coordination number. Assuming the coordination sphere to broaden symmetrically, this number is usually defined as an integral from zero to the average radius.

To estimate the number of bonds, let us express the integral in Eq. (23) in terms of the structure factor *S*(0), related to the compressibility by

$$S(0) = T(\partial n_a / \partial p)_T. \quad (24)$$

The structure factor *S*(0) is given by the integral

$$S(0) - 1 = 4\pi n_a \int_0^\infty [g(R) - 1] R^2 dR. \quad (25)$$

We next separate the first coordination sphere and divide the region of integration in Eq. (25) into two intervals. The integral from 0 to $2e^2/I$ is equal to the difference between the coordination number $2C$ and the average number of atoms whose cores are within the sphere of radius $2e^2/I$:

$$d = 2C - 8\zeta_0. \quad (26)$$

Expressing this integral from Eq. (25), we have

$$d = S(0) - 1 - 4\pi n_a \int_{2e^2/I}^\infty [g(R) - 1] R^2 dR. \quad (27)$$

This representation is convenient for estimating the coordination number.

For low atomic densities, the departure of *g*(*R*) from unity may be neglected at distances larger than $2e^2/I$. Then, dropping the integral on the right-hand side of Eq. (27) and using Eq. (26), we have

$$2C = 8\zeta_0 + S(0) - 1, \quad S(0) - 1 \ll 1.$$

This expression represents, in fact, the first terms of the expansion of the coordination number in the small difference *S*(0) - 1.

At the critical point, where *S*(0) diverges, the coordination number is finite, the divergence being cancelled by the last term on the right-hand side of Eq. (27). Using the limiting cases of the problem, we construct a Padé approximation for densities below the critical one, to obtain

$$d = \frac{d_c [S(0) - 1]}{d_c + S(0) - 1}, \quad (28)$$

where *d_c* is the value of *d* at the critical point. This parameter can be estimated from the experimental data on the coordination number of liquid mercury along the saturation line (Fig. 2). A linear approximation of the density dependence within the error band yields, at the critical density, a coordination number of 2.6 and *d_c* = 1. Then Eq. (28) takes the form

$$d = 1 - S^{-1}(0),$$

and the number of bonds per atom is

$$C = 4\zeta_0 + \frac{1}{2} [1 - S^{-1}(0)]. \quad (29)$$

Substituting Eq. (29) into Eq. (22) we obtain the total polarizability per atom as a function of the quantities ζ_0 and *S*(0) dependent on thermodynamic parameters:

$$\alpha = \left\{ z + \frac{16}{3} \zeta_0 + \frac{2}{3} [1 - S^{-1}(0)] \right\} \left(\frac{e^2}{I} \right)^3. \quad (30)$$

Recall that Eq. (30) has been obtained for densities below the critical value. The inverse structural factor $S^{-1}(0)$ here decreases with increasing density and grows with temperature. In particular, this behavior is described by the asymptotic near-critical expansion (for $|\Delta T/T_c| \ll |\Delta n_a/n_c|^{1/\beta}$) as¹²

$$S^{-1}(0) = D|\Delta n_a|^{\delta-1} + F\Delta T|\Delta n_a|^{\delta-(1/\beta)-1},$$

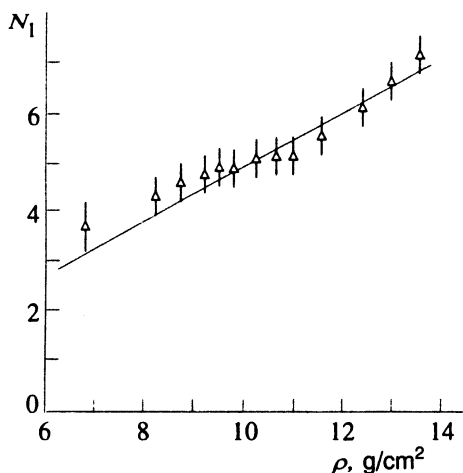


FIG. 2. Coordination number of extended liquid mercury along the saturation line (Ref. 13).

where $\Delta n_a = n - n_c$ and $\Delta T = T - T_c$ are thermodynamic parameters measured from the critical point, $\delta = 4.8$ and $\beta = 0.34$ are the critical exponents, and D and F are positive amplitudes. In contrast, the polarizability increases with density and decreases with increasing temperature.

The dielectric permittivity of an atomic gas is expressed in terms of the total atomic polarizability by using the Clausius-Mosotti equation or its regularized version

$$\epsilon_a = 1 + \frac{3\kappa(1 - \kappa^m)}{1 - \kappa}, \quad \kappa = \frac{4\pi}{3} n_a \alpha, \quad (31)$$

where $m - 1$ is the order of the successive approximation scheme in which the local field effect is described (the first-order effect being absent). The indeterminacy of the parameter m is important only near the pole of the Clausius-Mosotti equation, which formally corresponds to the limit $m \rightarrow \infty$. Actually, the approximation used need not be of too high order (say, not higher than third, which corresponds to $m = 4$; see Fig. 3). From the knowledge of the permittivity, it is easy to find the magnitude of the energy gap and to estimate the conductivity (Fig. 4). Note the qualitative agreement with experiment even though, due to the reduced ionization potential, the conductivity increases by more than a factor of 10^{10} compared to an ideal weakly ionized gas. However, below 4 g/cm^3 the nature of the density dependence is altered, presumably because of hole localization.

6. THERMOELECTRIC POWER

The sign of the majority charge carriers determines that of the Hall coefficient and thermoelectric power. Near the metal-nonmetal transition both are negative in accordance with the electronic character of conductance.⁵ However, at the liquid-gas critical point in mercury, the thermoelectric power vanishes and changes sign. In a certain density interval below the critical point, the positive sign of the thermoelectric power corresponds to hole conductance (Fig. 5). In

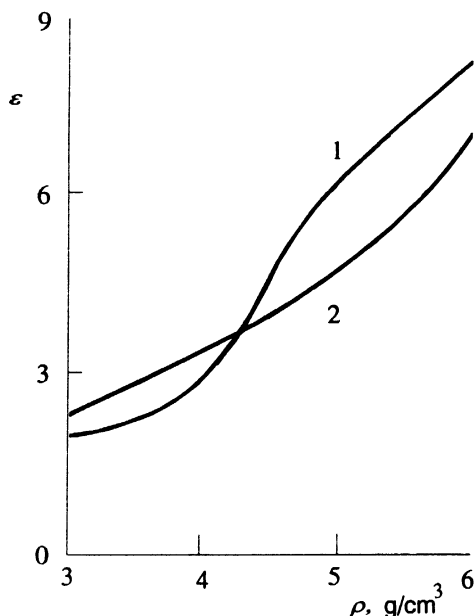


FIG. 3. Permittivity of mercury vapor versus density for $T = 1773 \text{ K}$. 1—experiment (Ref. 3). 2—regularized third-order Clausius-Mosotti equation.

fact, the observed change in the sign of the thermoelectric power is the only direct evidence to suggest electron-hole conductance.

The thermoelectric power can also be determined from the phenomenological expression for the energy flux associated with the electrical current in the system¹⁵

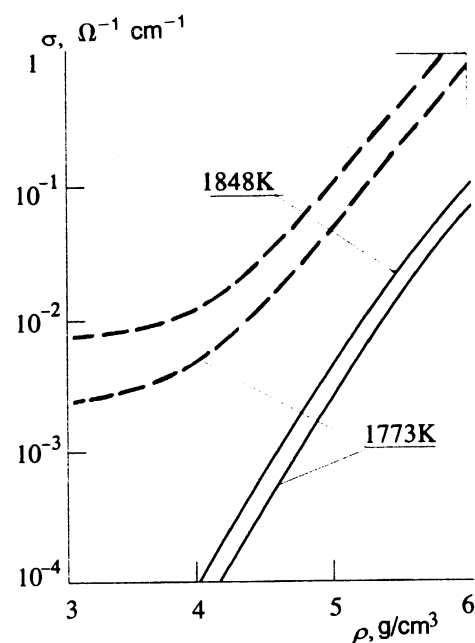


FIG. 4. Mercury vapor conductivity versus density for various temperatures. Dashed lines: experiment (Ref. 3); solid lines: theoretical estimate.

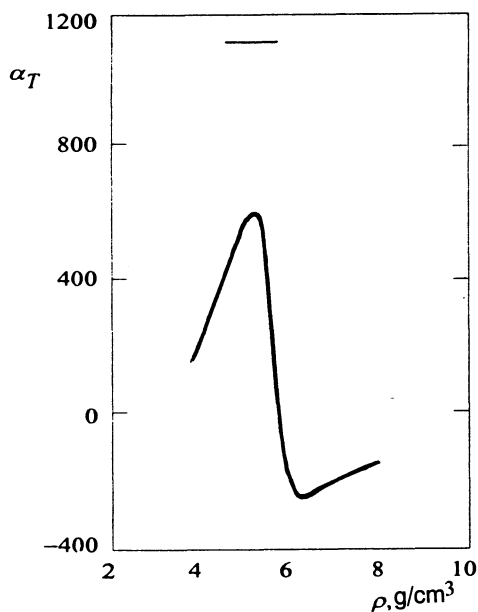


FIG. 5. Thermoelectric power of mercury for $T=1773$ K. The curve: experiment (Ref. 14) Hatching indicates the upper estimate corresponding to the hole conduction.

$$q = j(-\mu_e/e + \alpha_T T/k_B), \quad (32)$$

where q is the energy flux, j is the electrical current, α_T the thermoelectric power (in V/K), and k_B the Boltzmann constant. By definition, the energy flux due to the drift of electrons and holes is

$$q = \frac{j}{e} [-b_e(\Delta + \bar{\epsilon}_e) + b_h \bar{\epsilon}_h], \quad (33)$$

where b_e and b_h are the fractions of the electron and hole currents and $\bar{\epsilon}_e$ and $\bar{\epsilon}_h$ are the weighted average carrier energies as measured relative to the band bottom (the weight being proportional to the contribution to the current). By comparing Eqs. (32) and (33) and making use of the chemical potential formula, we obtain

$$\alpha_T = \frac{k_B}{eT} \left[\frac{\Delta}{2} (b_h - b_e) + b_h \bar{\epsilon}_h - b_e \bar{\epsilon}_e - \frac{T}{2} \ln \frac{a_e}{a_h} \right] \approx \frac{k_B \Delta}{2eT} (b_h - b_e), \quad \Delta \gg T. \quad (34)$$

From this it follows that whatever the electron-to-hole current ratio, the magnitude of the thermoelectric power is in the range from $-k_B \Delta/2eT$ to $k_B \Delta/2eT$ (Fig. 5). For equal electron and hole contributions the thermoelectric power (34) tends to zero. The relative contribution of the carriers depends, in particular, on their possible trapping by fluctuation clusters and bubbles. These questions necessitate a much more detailed analysis.

7. CONCLUSION

The study of the physical properties of mercury vapor near the liquid-gas critical point shows them to have typical semiconductor features. In particular, over a limited density interval electron-hole conduction may reasonably be suggested. In this interval the magnitude of the conductivity is primarily determined by the presence of a (density- and temperature-dependent) energy gap between the electron and conduction bands. Analysis also indicates a relation between the electron-hole conductance and the dielectric anomaly observed in the same parameter range. By determining the gap from a simple dielectric screening model it is possible to explain the extremely high conductivity of a dense mercury vapor compared with that for an ideal gas.

The most important factor limiting the applicability of the "uniform" dielectric screening model is the formation, and possibly even dominance, of cluster ions (cluster plasma). This alters plasma properties significantly; in particular, holes localize on the clusters. This being so, the marked semiconducting properties in a certain range of mercury parameters appear to be an exception rather than the rule for metal vapors. In conclusion, we emphasize the unique nature of highly nonideal ionized gaseous phases in metals: close to their liquid-gas transition points they may be either gaseous metals, or gaseous semiconductors, or a cluster plasma.

The work was carried out with the financial support of the International Science Fund (Grant No. MEK 000) and the Russian Fund for Fundamental Research (Grant No. 94-02-04170).

- ¹Ya. B. Zel'dovich and L. D. Landau, *Zh. Eksp. Teor. Fiz.* **14**, 32 (1944).
- ²N. F. Mott, *Metal-Insulator Transition*, Taylor and Francis, London (1991).
- ³F. Hensel, M. Stolz, G. Hohl, R. Winter, and W. Gotzloff, *J. Phys., Colloq.* **C5 1**, C5-191 (1991).
- ⁴J. M. Ziman, *Models of Disorder*, Cambridge University Press (1979).
- ⁵A. A. Likal'ter, *Usp. Fiz. Nauk* **162**, 119 (1992) [*Sov. Phys. Usp.* **35**, 591 (1992)].
- ⁶M. H. Cohen and J. Jortner, *Phys. Rev.* **10**, 978 (1974).
- ⁷A. A. Likal'ter, *Zh. Eksp. Teor. Fiz.* **94**, 157 (1988) [*Sov. Phys. JETP* **67**, 2478 (1988)].
- ⁸L. A. Turkevich and M. H. Cohen, *Phys. Rev. Lett.* **53**, 2323 (1984).
- ⁹L. J. Duckers and R. G. Ross, *Phys. Lett.* **A38**, 291 (1972).
- ¹⁰L. Friedman, *Philos. Mag.* **28**, 145 (1973).
- ¹¹A. F. Ioffe and A. R. Regel, *Prog. Semicond.* **4**, 237 (1960).
- ¹²L. D. Landau and E. M. Lifshitz, *Statistical Physics [in Russian]*, Nauka, Moscow, (1978), Pergamon, Oxford (1980), Part 2.
- ¹³K. Tamura and S. Hosokawa, *J. Non-Cryst. Solids* **156-158**, 646 (1993).
- ¹⁴F. Hensel, *J. Phys.: Condensed Matter* **2**, SA 33 (1990).
- ¹⁵L. D. Landau and E. M. Lifshitz, *Electrodynamics of Continua [in Russian]*, Pergamon, Oxford (1960).

Translated by E. Strelchenko

This article was translated in Russia and is reproduced here the way it was submitted by the translator, except for stylistic changes by the Translation Editor.